Contribution of synovial lining cells to synovial vascularization of the rat temporomandibular joint

Kayoko Nozawa-Inoue,[1] Fumiko Harada,[1] Jin Magara,[2] Atsushi Ohazama[1] and Takeyasu Maeda[1]

[1]*Division of Oral Anatomy, Niigata University Graduate School of Medical and Dental Sciences, Niigata, Japan*
[2]*Division of Dysphagia Rehabilitation, Niigata University Graduate School of Medical and Dental Sciences, Niigata, Japan*

Abstract

The lining layer of the synovial membrane in the temporomandibular joint (TMJ) contains two types of lining cells: macrophage-like type A and fibroblast-like type B cells. The type B cells are particularly heterogeneous in their morphology and immunoreactivity, so that details of their functions remain unclear. Some of the type B cells exhibit certain resemblances in their ultrastructure to those of an activated capillary pericyte at the initial stage of the angiogenesis. The articular surface, composed of cartilage and the disc in the TMJ, has few vasculatures, whereas the synovial lining layer is richly equipped with blood capillaries to produce the constituent of synovial fluid. The present study investigated at both the light and electron microscopic levels the immunocytochemical characteristics of the synovial lining cells in the adult rat TMJ, focusing on their contribution to the synovial vascularization. It also employed an intravascular perfusion with *Lycopersicon esculentum* (tomato) lectin to identify functional vessels *in vivo*. Results showed that several type B cells expressed desmin, a muscle-specific intermediate filament which is known as the earliest protein to appear during myogenesis as well as being a marker for the immature capillary pericyte. These desmin-positive type B cells showed immunoreactions for vimentin and pericyte markers (neuron-glial 2; NG2 and PDGFRβ) but not for the other markers of myogenic cells (MyoD and myogenin) or a contractile apparatus (αSMA and caldesmon). Immunoreactivity for RECA-1, an endothelial marker, was observed in the macrophage-like type A cells. The arterioles and venules inside the synovial folds extended numerous capillaries with RECA-1-positive endothelial cells and desmin-positive pericytes to distribute densely in the lining layer. The distal portion of these capillaries showing RECA-1-immunoreactivity lacked lectin-staining, indicating a loss of blood-circulation due to sprouting or termination in the lining layer. The desmin-positive type B and RECA-1-positive type A cells attached to this portion of the capillaries. Some capillaries in the lining layer also expressed ninein, a marker for sprouting endothelial cells, called tip cells. Since an activated pericyte, macrophage and tip cell are known to act together at the forefront of the vessel sprout during angiogenesis, the desmin-positive type B cell and RECA-1-positive type A cell might serve as these angiogenic cells in the synovial lining layer. Tomato lectin perfusion following decalcification would be a highly useful tool for research on the vasculature of the mineralized tissue. Use of this technique combined with immunohistochemistry should permit future extensive investigations on the presence of the physiological angiogenesis and on the function of the lining cells in the synovial membrane.

Key words: angiogenesis; synovial lining cell; synovial membrane; temporomandibular joint; tomato lectin.

Introduction

The synovial membrane in the temporomandibular joint (TMJ) consists of a connective tissue sublining layer and a cellular lining called the synovial intima or the lining cell layer. Ultrastructurally, the synovial lining cells in the TMJ are divided into two types: macrophage-like type A and fibroblast-like type B cells (Nozawa-Inoue et al. 2003), as reported in other systemic joints (Graabæk, 1982, 1984; Iwanaga et al. 2000). The type A cell has morphological and immunocytochemical characteristics indicating a macrophage lineage with phagocytic activity. Another lining cell, the fibroblast-like type B cell, possesses a well-developed rough endoplasmic reticulum (rER), long cytoplasmic projections, surrounding basement membrane-like structure, and cell membrane caveolae, although it is heterogeneous in its

morphology and immunoreactivity (Nozawa-Inoue et al. 2003). The heterogeneity of the lining cells continues to generate controversy concerning the presence of the third cell type (Nishijima, 1981; Alvez et al. 2014); hence, their detailed origin and functional significance remain unclear. We confirmed an intense expression of caveolin-1 in the caveolae of the type B cell by immunocytochemistry using an antibody to the 25-kDa heat shock protein (Hsp25) that is a marker of the type B cells (Nozawa-Inoue et al. 1999, 2006). Interestingly, the caveolin-1-positive caveolae additionally exhibited muscle-specific caveolin-3-reactivity in some of the type B cells (Nozawa-Inoue et al. 2007). The cardiac muscle and certain types of smooth muscle express both caveolin-1 and -3; however, non-muscle cells containing these two caveolins have been restricted to three region-specific cells – the astroglial cell (Ikezu et al. 1998), sinus endothelial cells in the spleen (Uehara & Miyoshi, 2002), and chondrocytes in the limb cartilage (Schwab et al. 1999, 2000).

The synovial sublining layer is richly equipped with fenestrated blood capillaries (Izutsu, 1986; Nozawa-Inoue et al. 1998) which produce a constituent of the synovial fluid. The rheumatoid arthritis (RA) synovium is marked by neovascularization at the early stage, with subsequent infiltration of inflammatory cells and pannus formation. Since the newly formed blood capillaries contribute to the development and progress of RA, angiogenesis in the synovium has been considered a therapeutic target for the disease (Koch, 2000; Bainbridge et al. 2006; Semerano et al. 2011). Post-natal angiogenesis rarely occurs except in the female reproductive organ or hypoxic tissue under pathologic conditions such as tumor growth and wound healing. On the other hand, mechanical tensile force has been reported to be an angiogenic inducer in the skin (Erba et al. 2011). In the TMJ, the articular surface – including the cartilage and disc – has few vasculatures, and the synovial membrane is repeatedly stretched due to jaw movement arising from mandibular rotation and sliding. These facts and the situation in the TMJ lead us to the hypothesis that physiological angiogenesis might be elicited in the mature synovial membrane. However, no blood vessel sprouting in the synovial membrane under normal conditions has yet been confirmed.

During the angiogenic process, the pericytes of the pre-existing blood capillary are activated and detached from the vessel walls at the forefront of the sprouts (Díaz-Flores et al. 2009). The activated pericyte bears certain resemblances to the fibroblast-like type B cell in its morphology, such as a bulging cytosol, numerous ribosomes, rER, micropinocytic vesicles, and a fragmented basement membrane (Díaz-Flores et al. 2009). Another specialized endothelial cell, called the tip cell, is sent out from the vessels and guides the direction of the newly formed sprout (Geudens & Gerhardt, 2011). At the site where two neighboring tip cells make contact via their filopodia, macrophages act as bridge cells to assist them in accurate fusion (Fantin et al. 2010). The intravascular perfusion of *Lycopersicon esculentum* lectin (tomato lectin) is a simple staining method to visualize the blood-circulating vessel *in vivo* (Ezaki et al. 2001); it is often used for observation of the angiogenic process in the brain (Xu et al. 2004), kidney (Basile et al. 2011; Rymer et al. 2014), and soft tissue tumors (Morikawa et al. 2002; Inai et al. 2004). This method labels only perfused (functional) vessels, whereas immunohistochemical endothelial markers such as CD31 are further bound to the unfunctional sprouting, or terminating vessels on the tissue sections. Therefore, angiogenic cells – including an activated pericyte and an endothelial tip cell at the vessel sprout – can be identified respectively as pericyte and endothelial marker-positive cells associating with the lectin unperfused portion of capillaries. There is, however, no report which demonstrates functional or sprouting vessels using the intravascular lectin-injection technique in the mature synovial joint *in vivo*.

Desmin, a major muscle-specific intermediate filament, is the earliest protein to appear during myogenesis (Paulin & Li, 2004). The vascular smooth muscle cell also expresses desmin, caveolin-1, caveolin-3, and α-smooth muscle actin (αSMA), but developing pericytes involved in the capillary sprouting lack αSMA (Nehls et al. 1992). The present study was therefore undertaken to examine: (i) an expression of the desmin in the fibroblast-like type B cell in mature rat TMJ by immunocytochemistry at both light and electron microscopic levels; (ii) further immunohistological characteristics of the type B cells using the markers for the intermediate filaments (vimentin and nestin), smooth muscle cells (αSMA and caldesmon), myogenic cells (myogenin and MyoD), and capillary pericytes (neuron-glial 2; NG2 and PDGFRβ); and (iii) *in vivo* synovial vascularity by intravascular tomato lectin perfusion following fluorescent immunolabeling using endothelial cell marker RECA-1 (rat endothelial cell antigen-1; Duijvestijn et al. 1992) and tip cell marker ninein (Matsumoto et al. 2008) on the decalcified whole TMJ specimen. Finally, the occurrence of physiological angiogenesis in the synovial membrane and the contribution of the synovial lining cells to the vasculature are discussed.

Materials and methods

Animals and tissue preparation

Male 8-week-old Wistar rats ($n = 8$) were purchased from Charles River Laboratories Japan. Under anesthesia by an intraperitoneal injection of 8% chloral hydrate (300 mg kg^{-1}), the animals were perfused with a fixative containing 4% paraformaldehyde and 0.025% glutaraldehyde in a 0.067 M phosphate buffer (pH 7.4) through the left ventricle. The removed heads were decalcified with a 10% ethylene diamine tetra-acetic acid disodium (EDTA-Na$_2$) solution for 4 weeks at

4 °C. After decalcification, the TMJ were removed *en bloc*, equilibrated in a 30% sucrose solution for cryoprotection, and embedded in OCT compound (Tissue-Tek®; Sakura Finetechnical, Tokyo, Japan). Serial sagittal cryosections including the TMJ were cut at a thickness of 7 or 25 μm in a cryostat (CM3050S; Leica Microsystems, Nussloch, Germany) and mounted onto silane-coated glass slides. All experiments were performed under the guidelines of the Niigata University Intramural Animal Use and Care Committee (approval number 26, 82-1).

Light- and electron-microscopic immunohistochemistry

Information on the primary antibodies used in this study is given in Table 1. The cryostat sections were processed for the immunohistochemical detection of desmin or RECA-1 by light and electron microscopy using a commercially available avidin-biotin-complex (ABC) kit (Vector Lab. Inc., Burlingame, CA, USA). After inhibition of endogenous peroxidase with an absolute methanol containing 0.3% H_2O_2 for 20 min, the sections (25 μm thick) were immersed with 2.5% normal horse serum (Vector Lab.) for 60 min at room temperature. They were reacted overnight at 4 °C with either a desmin or a RECA-1 monoclonal antibody diluted with 0.01 M phosphate-buffered saline (PBS). The bound primary antibody was then localized using a biotinylated anti-mouse IgG (1 : 100; Vector Lab.) and subsequently with ABC conjugated with peroxidase (Vector Lab.) for 90 min each at room temperature. Final visualization used 0.04% 3,3′-diaminobenzidine tetrahydrochloride (DAB) and 0.002% H_2O_2 in a 0.05 M Tris–HCl buffer (pH 7.6). Immunoreacted sections were counter-stained with 0.03% methylene blue.

Some immunostained sections without counter-staining were post-fixed in 1% OsO_4 (TAAB Laboratories Equipment Ltd, England) reduced with 1.5% potassium ferrocyanide for 1 h at 4 °C, dehydrated in an ascending series of ethanol, and finally embedded in epoxy resin (Plain Resin; Nissin EM, Tokyo, Japan). Plastic sections (1 μm thick) were stained with 0.03% methylene blue. Ultrathin sections (70 nm thick) were briefly double-stained with uranyl acetate and lead citrate and examined in a transmission electron microscope (H-7650; Hitachi Co. Ltd, Tokyo, Japan).

Double fluorescent immunostaining

For fluorescent double-labeling immunocytochemistry, sections (7 μm thick) were incubated with either the mouse monoclonal or rabbit polyclonal antibody to desmin as a first primary antibody, followed by fluorescein isothiocyanate (FITC)- or Texas Red™- conjugated anti-mouse or -rabbit IgG (1 : 100; Vector Lab.). They were further reacted with a second primary antibody to either marker protein shown in Table 1, and a subsequent species-specific second antibody which was of a different color than the primary one. The double-labeled sections were cover-slipped with a Vectashield® mounting medium with 4′,6-diamidino-2-phenylindole (DAPI; Vector Lab.) to stain the nuclei and finally examined in a fluorescence microscope (AxioImazer M; Carl Zeiss, Jena, Germany).

Immunocytochemical controls were performed by: (1) replacing the primary antibodies with non-immune sera or PBS and (2) omitting the second antibodies. These control sections did not reveal any immunoreaction.

Lectin perfusion

Following the protocol of Basile et al. (2011), another three animals were intravenously injected with fluorescein *L. esculentum* lectin (tomato lectin)(Vector Lab; 0.125 mg 100 g^{-1} body weight) via the jugular vein; the lectin was allowed to circulate before fixation under the same anesthesia as described above. Five minutes later, they were perfused with 4% paraformaldehyde (pH 7.4). The heads were removed and decalcified in a dark box in the same manner as described above. Frozen sections of the TMJ embedded in OCT compound were cut at 35–50 μm in a cryostat and mounted onto silane-coated glass slides. The lectin-stained sections were processed for immunohistochemistry using Texas Red™-labeled antibodies to desmin, RECA-1 or ninein. PBS containing 0.3% Triton-X-100 (Wako Pure Chemical Industries, Osaka, Japan) was used for rinsing and dilution of the antibodies instead of ordinary PBS. The sections were cover-slipped with a mounting medium containing DAPI and examined with a confocal laser scanning microscope (LSM 700; Carl Zeiss). Confocal z-stack images were obtained by software ZEN 2009 (Carl Zeiss) which automatically calculates the

Table 1 List of primary antibodies.

Antibody	Host species	Company	Dilution
Desmin	Mouse monoclonal (clone D33)	Dako, Glostrup, Denmark	1 : 200
	Rabbit polyclonal	Thermo Fisher Scientific Inc., Waltham, MA, USA	1 : 800
Hsp25	Rabbit polyclonal	Stressgen Biotechnologies Corp., Victoria, Canada	1 : 5000
RECA-1	Mouse monoclonal (clone HIS52)	AbD Serotec, Kidlington, UK	1 : 100
Vimentin	Mouse monoclonal (clone V9)	Sigma-Aldrich, St. Louis, MO, USA	1 : 4000
Nestin	Mouse monoclonal (clone Rat-401)	Chemicon Int. Inc., Temecula, CA, USA	1 : 2000
αSMA	Rabbit polyclonal	Novus Biologicals, Inc., Littleton, CO, USA	1 : 400
Caldesmon	Rabbit polyclonal	Santa Cruz Biotechnology, Inc., Dallas, TX, USA	1 : 500
Myogenin	Mouse monoclonal (clone F50)	Dako, Glostrup, Denmark	1 : 500
MyoD	Rabbit polyclonal	Santa Cruz Biotechnology, Inc., Dallas, TX, USA	1 : 500
NG2	Mouse monoclonal (clone132.38)	Santa Cruz Biotechnology, Inc., Dallas, TX, USA	1 : 500
PDGFRβ	Rabbit monoclonal (clone 28E1)	Cell Signaling Technology Japan K.K., Tokyo	1 : 50
Ninein	Rabbit polyclonal	Bioss, Inc., Woburn, MA, USA	1 : 300

recommended z-interval thickness and the number of the slices according to the emission wavelength, objective lens, and the pinhole diameter.

Results

Immunolocalization of desmin in rat TMJ

The synovial lining cells and the muscles – including smooth muscle cells of the vessel wall – exhibited intense immunoreactions for desmin (Fig. 1A,B). The synovial lining layer consisted of desmin-positive and -negative lining cells (Fig. 1C). Ultrastructurally, desmin-immunopositive lining cells possessed well-developed rER, a long cytoplasmic process, numerous cell membrane caveolae, and surrounding basement membrane-like structures (Fig. 1D,E), suggesting that they were fibroblast-like type B cells. In addition, double-labeling immunohistochemistry for desmin and Hsp25, which is a pan-type B cell marker, demonstrated their co-localization
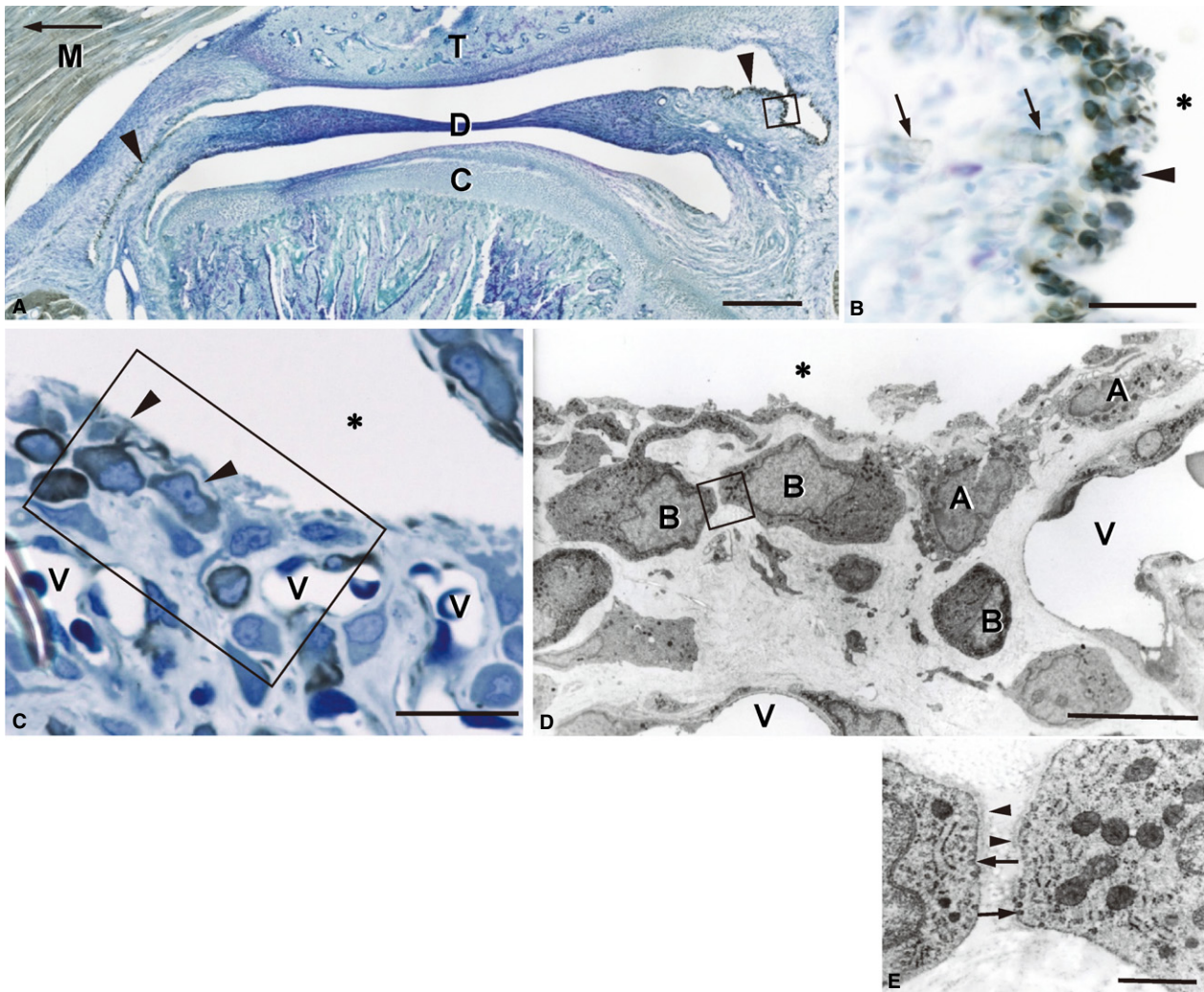

Fig. 1 Desmin immunoreactivity in the rat TMJ. (A) Frozen sagittal section, 25 μm thick, counter-stained with methylene blue. An arrow indicates the anterior direction. Intense immunoreactivity is observed in the synovial membrane (arrowheads) and the skeletal muscle (M). C, mandibular condyle; D, articular disc; T, temporal bone. (B) Higher magnification of the boxed area in (A). The synovial lining cells exhibit strong immunoreactions (arrowhead). The capillary pericytes (arrows) are also immunopositive. (C) Desmin immunoreactivity in the synovial lining cells. Plastic section, 1 μm thick. Desmin immunoreactions are localized in the cytoplasm of the lining cells (arrowheads). The synovial lining layer consists of immunopositive and negative lining cells. Note the numerous blood capillaries (V) near the lining cells. (D) An immunoelectron micrograph of the boxed area in (C). Immunonegative lining cells (A) contain lysosomes and develop filopodia-like surface folds, indicating that they are macrophage-like type A cells. Immunopositive cells (B) possess well-developed rER, a large nucleus, and a long cytoplasmic process, all of which are characteristic features of the fibroblast-like type B cell. (E) Higher magnification of the boxed area in D. The caveolae (arrows) and basement membrane-like structures (arrowheads) are seen around both of the type B cells. *Articular cavity. Scale bars: 500 μm (A), 200 μm (B), 50 μm (C), 10 μm (D), 1 μm (E).
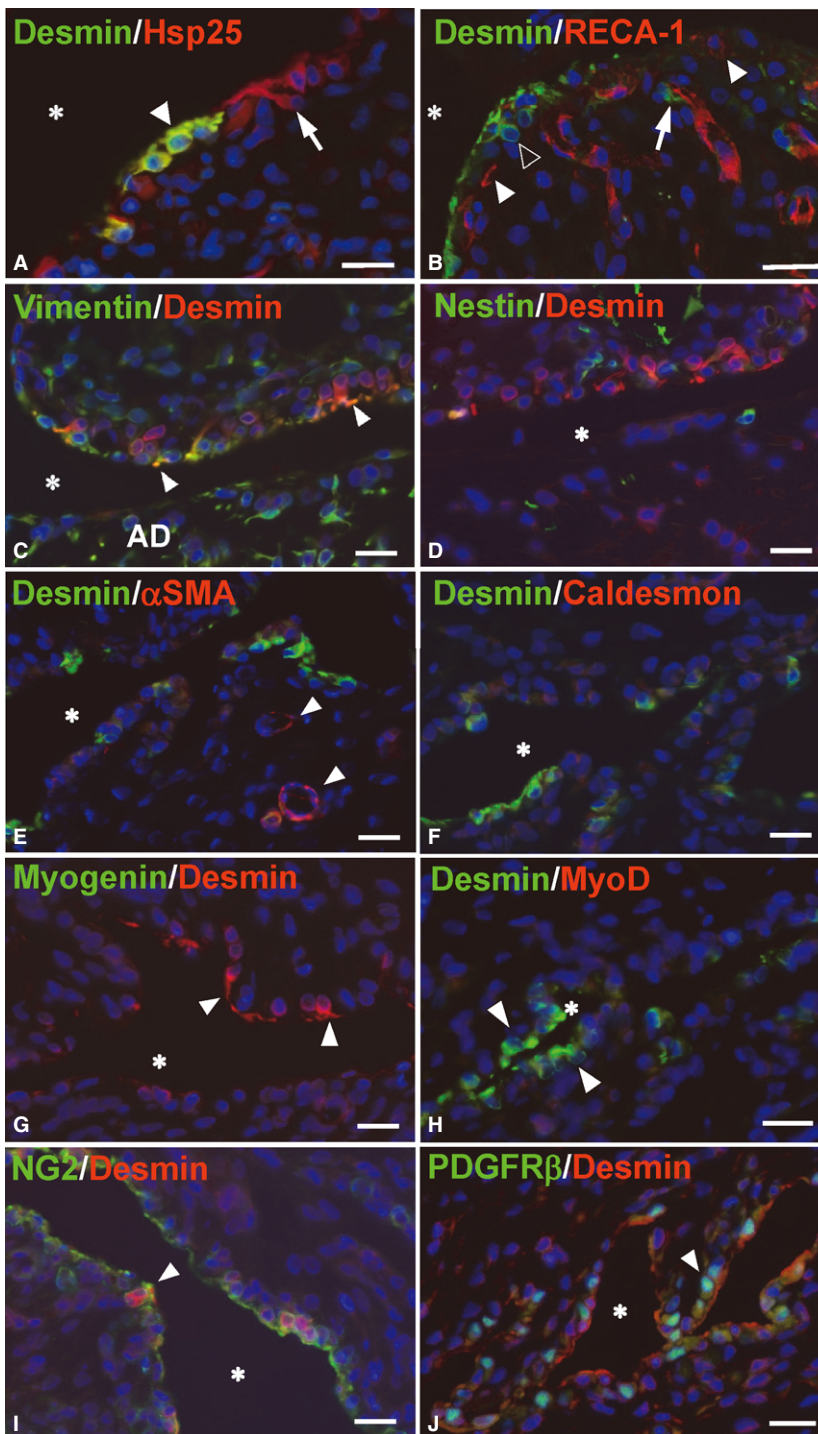
Fig. 2 Fluorescence microscope images of double-labeling sections for desmin and either specific marker. Frozen section, 7 μm thick, nuclei stained with DAPI (blue). *Articular cavity. (A) All desmin-positive type B cells show Hsp25-immunoreactions (arrowhead, yellow). Some Hsp25-positive cells (arrow, red) are negative for desmin. (B) RECA-1-positive (red) endothelial cells exhibit the tubular profile of the blood vessels with a desmin-positive (green) pericyte (arrow). The synovial lining layer consists of RECA-1-positive type A cells (white arrowheads) and desmin-positive type B cells (black arrowhead). (C,D) Desmin and intermediate filament proteins. Several desmin-positive B cells (red) show vimentin-immunoreactions (green), especially in their cytoplasmic processes (arrowheads, yellow). The cells in the articular disc (AD) show a strong immunoreaction for vimentin, but not for desmin. Nestin-immunoreaction (green) is rarely co-localized with desmin (red). (E,F) Desmin and the markers for smooth muscle cells. αSMA- and caldesmon-immunoreactivity (red) are not perceptible in the synovial lining cells. Intense αSMA reactions are only localized in the smooth muscle cells surrounding the blood vessels (arrowheads). (G,H) Desmin and the markers for the myogenic cells. Desmin-positive type B cells (arrowheads) lack myogenin (green) and myoD (red). (I,J) Desmin and the markers for the blood capillary pericytes. The desmin-positive B cells (red) show NG2 immunoreactivity around their cell membrane (arrowhead). PDGFRβ immunoreactions are localized in the nuclei of several desmin-positive cells (arrowhead). Scale bars: 20 μm.

in the fibroblast-like type B cells (Fig. 2A). The macrophage-like type A cells, which had lysosomes and surface folds like filopodia, did not show any desmin-immunoreaction (Fig. 1D). It was noteworthy that numerous blood capillaries lay closely beneath or among the lining cells (Fig. 1C).

Double staining of desmin and either marker for the other intermediate filaments, smooth muscle cells, myogenic cells, capillary pericytes or endothelial cells

The immunoreaction of desmin was co-localized with an intermediate filament vimentin but not nestin in the

fibroblast-like type B cells (Fig. 2C,D). The desmin-positive B cells were negative for the markers of a contractile apparatus (αSMA and caldesmon) (Fig. 2E,F), myogenic cells (myogenin and MyoD) (Fig. 2G,H), and endothelial cells (RECA-1) (Fig. 2B), but they were positive for the capillary pericyte markers, NG2 and PDGFRβ (Fig. 2I,J).

Immunoelectron microscopy for RECA-1-positive synovial cells

RECA-1-immunoreactions were localized in the endothelial cells and several lining cells (Fig. 3A). Immunoelectron microscopy of the RECA-1-positive lining cells revealed their filopodia-like surface folds and lysosomes, indicating them to be macrophage-like type A cells (Fig. 3B). The fibroblast-like type B cells lacked RECA-1.

Lectin-stained functional blood vessels in the TMJ

The synovial membrane and bone marrow in both the mandible and temporal bone were well supplied with lectin-stained vasculature, whereas only a few lectin-perfused vessels were seen on the surface of the condylar cartilage and intermediate zone of the articular disc (Fig. 4A). In the mandibular condyle, RECA-1-positive endothelial cells without lectin-staining localized at the edge of the cartilage matrix, suggesting that they were the unperfused forefront of the vascular invasion into the cartilage from the bone marrow (Fig. 4B; see Supporting Information Fig. S1).

Relationship between synovial lining cells and the blood capillaries

Confocal laser scanning microscopy provided clear images of the rich vascularity in the synovial folds (Fig. 5). The lectin-stained (blood-circulating) arterioles and venules inside the synovial fold extended numerous small capillaries toward the surface of the synovial membrane. In the synovial lining layer, these perfused capillaries with RECA-1-immunoreaction were densely distributed among the synovial lining cells (Fig. 5A). A few RECA-1-positive

endothelial cells localized at the peripheral part of the capillaries lost the lectin-staining (white arrowheads in Fig. 5B), indicating a loss of blood circulation. These unperfused portions of the capillaries lay adjacent to the articular cavity accompanying the macrophage-like type A cells with a RECA-1-immunoreaction (black arrowheads in Fig. 5B).

The desmin-positive pericytes were circumferentially arranged on the perfused arterioles and venules, whereas the distal part of the capillaries had a few irregularly arranged pericytes (Fig. 5C). At the most peripheral portion of the capillaries in the synovial lining layer, the desmin-positive cells were loosely associated with the endothelium, extending their cytoplasmic processes in multiple directions, suggesting they were desmin-positive type B cell (Fig. 5C, D).

Several lectin-stained capillaries in the synovial lining layer expressed dot-like immunoreactions for ninein – the tip cell marker (Fig. 5E).

Discussion

The intravascular injection of tomato lectin enabled the representation of functional vessels in all the components of TMJ *in vivo*. This is the first report to use a decalcified frozen section after lectin perfusion in the mineralized organ such as articulation. Previously, an India ink or acrylic resin injection often was employed to visualize the vasculature experimentally; however, these methods do not always represent the functional vessels *in vivo*. The tomato lectin entered the blood flow in a living animal, whereas both ink and resin were intravascularly injected after the perfusion with a fixative. In addition, neither the ink- nor the resin-injected samples could be used for immunohistochemistry. These former methods were accordingly insufficient for investigating the details of the relationship between angiogenesis and its associated cells *in vivo*. The capillary labeling by tomato lectin injection has been reported to be a sensitive and reliable method of visualizing vascularity in various soft tissues including the brain, kidney, liver, intestine, spleen, skin, muscle, and experimental tumors (Morikawa et al. 2002; Robertson et al. 2015). We confirmed that the

Fig. 3 RECA-1-immunoreactivity in the synovial membrane. (A) RECA-1-reactions are localized in the endothelial cells (arrows) of the capillaries (V) and several lining cells (arrowheads). (B) An immunoelectron micrograph of the boxed area in (A). Immunopositive lining cells (A) possess filopodia-like surface folds, indicating macrophage-like type A cells. Type B cells (B) are immunonegative. *Articular cavity. Scale bars: 20 μm (A), 4 μm (B).
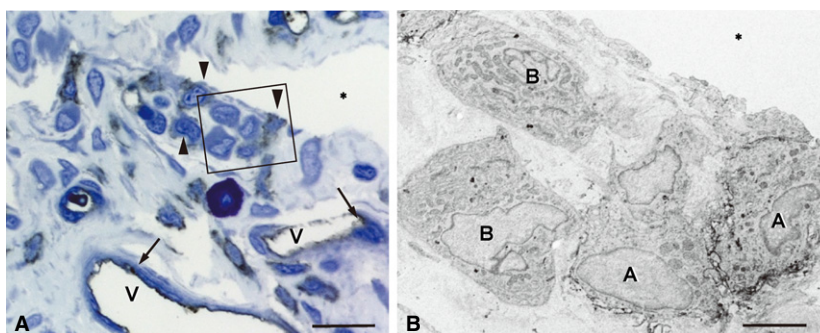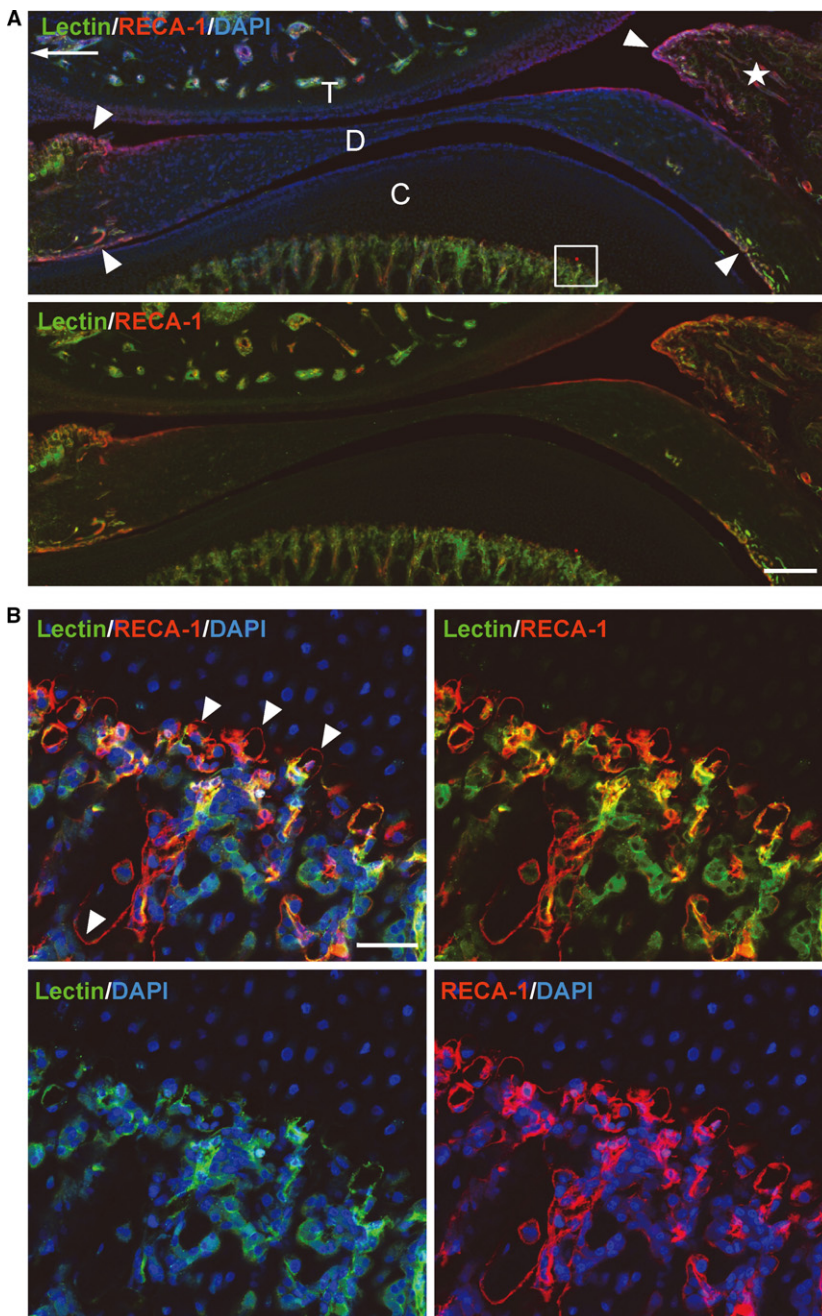
Fig. 4 A section of tomato lectin (green) perfused TMJ, co-labeled with RECA-1 (red). Frozen sagittal section, 40 μm thick, nuclei stained with DAPI (blue). (A) An arrow indicates the anterior direction. The synovial membrane (arrowheads) and bone marrow are well supplied with vasculature, whereas the intermediate zone of the disc (D) and the surface of the condylar cartilage (C) have few vessels with lectin affinities. T, temporal bone. (B) Magnified view of the boxed area in (A). RECA-1-positive endothelial cells without lectin-staining (arrowheads) accumulate at the edge of the cartilage matrix in the mandibular condyle. Scale bars: 200 μm (A), 50 μm (B).

tomato lectin was tightly bound to the endothelia even after subsequent decalcification; therefore, the cryosections including whole joint were utilized for further immunohistochemistry. This method would be a highly useful tool for research on mineralized tissue such as the teeth, bone, and particularly articulation to evaluate the participation of vessel invasion in endochondral ossification, or vessel proliferations in RA pannus formation.

Desmin-positive synovial lining cells, which were immunocytologically classified as fibroblast-like type B cells, expressed capillary pericyte marker proteins NG2 and PDGFRβ, but lacked αSMA in this study. In pericyte differentiation models such as an experimentally induced angiogenesis in mesentery (Nehls et al. 1992) and developing rat retina (Hughes & Chan-Ling, 2004), pericyte precursor cells (developing pericytes) were negative for αSMA but were clearly reactive for desmin. An activated pericyte or a transitional cell between the activated pericyte and fibroblast – which is localized at the front of the capillary sprouts – is known to participate in angiogenesis by determining the sprouting location and by guiding newly formed vessels (Nehls et al. 1992; Tsuzuki & Sasa, 1994; Morikawa et al. 2002; Ozerdem & Stallcup, 2003; Díaz-Flores et al. 2009). These angiogenic phenotypes of the pericyte bore a
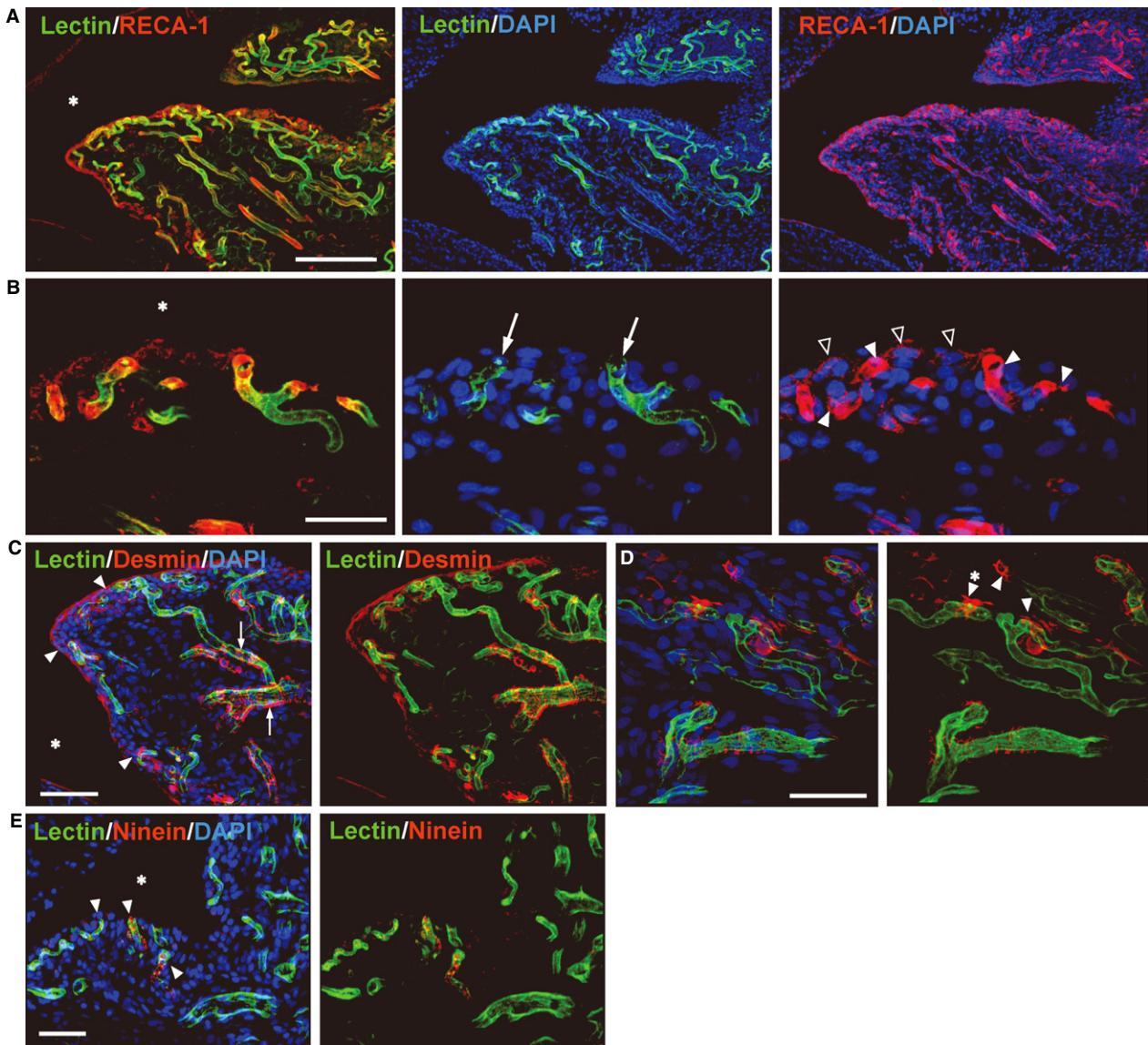
Fig. 5 (A) Confocal microscopic images of the synovial fold (✭ in Fig. 4A). Frozen sagittal sections, 40 μm thick, tomato lectin (green) perfused, co-labeled with RECA-1 (A,B), desmin (C,D) or ninein (E) (red), nuclei stained with DAPI (blue). * Articular cavity. (A) The lectin-perfused arterioles and venules with RECA-1-positive endothelial cells send out numerous capillaries toward the surface of the synovial membrane. These capillaries are distributed densely in the synovial lining layer. The RECA-1-immunoreactive cells without lectin-staining that localize along the surface of the synovium are the macrophage-like type A cells. (B) Higher magnification of the synovial lining layer. Small perfused capillaries (arrows) exist adjacent to the articular cavity. The RECA-1-immunoreactive endothelial cells (white arrowheads) at the peripheral portion lack lectin-staining. The macrophage-like type A cells with RECA-1-immunoreaction (black arrowheads) attach to this unperfused portion of the capillaries. (C) The desmin-positive pericytes are circumferentially arranged (arrows) on the perfused arterioles and venules, whereas the peripheral capillaries have a few irregularly arranged pericytes. At the distal end of the capillaries, the desmin-positive type B cells (arrowheads) are loosely associated with the endothelium, and extend their cytoplasmic processes in multiple directions. (D) The desmin-positive type B cells with the cytoplasmic projections (arrowheads) localize around the edge of the capillaries. (E) Immunoreactions for ninein (arrowheads) localized in the peripheral capillaries and lining layer. Scale bars: 200 μm (A), 40 μm (B), 50 μm (C–E).

resemblance to desmin-positive type B cells in their morphology, including a large and ovoid nucleus with prominent nucleoli, abundant rER, ribosome, Golgi complex, slender mitochondria in the bulged cytoplasm, and the basement membrane-like structure (Nozawa-Inoue et al. 2003; Díaz-Flores et al. 2009). In addition to these immunohistological and morphological correspondences, the existence of numerous capillaries with the lining cells in the synovial lining layer implies that the desmin-positive type B cells might contribute to the angiogenesis as activated pericytes.

During the initial phase of angiogenesis, pre-existing vessels send out specialized endothelial cells called tip cells as

well as activated pericytes (Geudens & Gerhardt, 2011). The tip cell scans the environment for attracting or repelling signals with its filopodia, and so serves to guide the new vessel in a certain direction. At the site where two tip cells make contact via their filopodia, tissue macrophages elicit and stabilize their contact as bridge cells (Fantin et al. 2010). The facilitation of activated pericytes being dissociated from the pre-existing capillary by macrophages has been also suggested (Díaz-Flores et al. 2009). In the present study, the distal end of the RECA-1-reactive endothelium lacked lectin-staining in the synovial surface, indicating a lack of blood circulation due to vessel sprouting or obliteration. The RECA-1-positive macrophage-like type A cells and desmin-positive type B cells were localized adjacent to such unperfused portions. It is further noteworthy that several capillaries at such a site expressed ninein, the angiogenic tip cell marker (Matsumoto et al. 2008). These findings suggest that so-called synovial lining cells – macrophage-like type A and fibroblast-like type B – which show heterogeneity in their immunocytological characteristics might contain angiogenic cells. It seems reasonable to assume that the desmin-positive type B cell contributes to angiogenesis in the synovial lining layer as an activated pericyte, and the RECA-1-positive type A cell functions together as a tip cell or macrophage.

To our knowledge, there has been no report on the occurrence of physiological angiogenesis in the synovial membrane under normal conditions, whereas numerous investigations are available on the vessels in the RA synovium. In a comparative study of the arthropathy and unaffected control synovium, the normal synovial cells had vascular endothelial growth factor (VEGF) polypeptide and mRNA, although at lower expressions than those of RA (Nagashima et al. 1995) and chondromatosis (Li et al. 2014). Like the capillaries in our observations, the pericyte-uncoated vessels were unstable or immature and responsive to the angiogenic signals like VEGF (Jain, 2001; Gee et al. 2003). Furthermore, we found that the first appearance of the desmin- and RECA-1-positive lining cells preceded the vasculogenesis in the synovial lining layer during the development of the rat TMJ (see Supporting Information Fig. S2). RECA-1-positive endothelial cells with desmin-positive pericytes successively formed capillaries in the synovial lining layer after completion of the articular cavity, and the capillaries accompanying RECA-1 or desmin-positive lining cells gradually increased in number and size. These facts also support the possibility of physiological angiogenesis with the guidance of certain lining cells in the mature healthy synovium. An understanding of the structure and function of the synovial cells and vasculature in the normal synovium is important to make progress in the vascular targeting treatment of arthritis. Further studies focusing on physiological angiogenesis in the synovium are necessary to determine the contribution of the synovial lining cells to the capillary sprouting.

Author contributions

Study conception and design: K.N-I. Acquisition of data: K.N-I., F.H., J.M. Analysis and interpretation of data: K.N-I., A.O., T.M. Drafting of manuscript: K.N-I. Critical revision: A.O., T.M.

Conflict of interest

The authors declare no conflict of interest.

References

Alvez CS, de Carvalho Moraes LO, Marques SR, et al. (2014) Analysis by light, scanning, and transmission microscopy of the intima synovial of the temporomandibular joint of human fetuses during the development. *Anat Res Int* **2014**, 732720. http://doi.org/10.1155/2014/732720.

Bainbridge J, Sivakumar B, Paleolog E (2006) Angiogenesis as a therapeutic target in arthritis: lessons from oncology. *Curr Pharm Des* **12**, 2631–2644.

Basile DP, Friedrich JL, Spahic J, et al. (2011) Impaired endothelial proliferation and mesenchymal transition contribute to vascular rarefaction following acute kidney injury. *Am J Physiol Renal Physiol* **300**, F721–F733.

Díaz-Flores L, Gutiérrez R, Madrid JF, et al. (2009) Pericytes. Morphofunction, interactions and pathology in a quiescent and activated mesenchymal cell niche. *Histol Histopathol* **24**, 909–969.

Duijvestijn AM, van Goor H, Klatter F, et al. (1992) Antibodies defining rat endothelial cells: RECA-1, a pan-endothelial cell-specific monoclonal antibody. *Lab Invest* **66**, 459–466.

Erba P, Miele LF, Adini A, et al. (2011) A morphometric study of mechanotransductively induced dermal neovascularization. *Plast Reconstr Surg* **128**, 288e–299e.

Ezaki T, Baluk P, Thurston G, et al. (2001) Time course of endothelial cell proliferation and microvascular remodeling in chronic inflammation. *Am J Pathol* **158**, 2043–2055.

Fantin A, Vieira JM, Gestri G, et al. (2010) Tissue macrophages act as cellular chaperones for vascular anastomosis downstream of VEGF-mediated endothelial tip cell induction. *Blood* **116**, 829–840.

Gee MS, Procopio WN, Makonnen S, et al. (2003) Tumor vessel development and maturation impose limits on the effectiveness of anti-vascular therapy. *Am J Pathol* **162**, 183–193.

Geudens I, Gerhardt H (2011) Coordinating cell behaviour during blood vessel formation. *Development* **138**, 4569–4583.

Graabæk PM (1982) Ultrastructural evidence for two distinct types of synoviocytes in rat synovial membrane. *J Ultrastruct Res* **78**, 321–339.

Graabæk PM (1984) Characteristics of the two types of synoviocytes in rat synovial membrane. *Lab Invest* **50**, 690–702.

Hughes S, Chan-Ling T (2004) Characterization of smooth muscle cell and pericyte differentiation in the rat retina in vivo. *Invest Ophthalmol Vis Sci* **45**, 2795–2806.

Ikezu T, Ueda H, Trapp BD, et al. (1998) Affinity-purification and characterization of caveolins from the brain: differential expression of caveolin-1, -2, and -3 in brain endothelial and astroglial cell types. *Brain Res* **804**, 177–192.

Inai T, Mancuso M, Hashizume H, et al. (2004) Inhibition of vascular endothelial growth factor (VEGF) signaling in cancer causes loss of endothelial fenestrations, regression of tumor vessels, and appearance of basement membrane ghosts. *Am J Pathol* **165**, 35–52.

Iwanaga T, Shikichi M, Kitamura H, et al. (2000) Morphology and functional roles of synoviocytes in the joint. *Arch Histol Cytol* **63**, 17–31.

Izutsu R (1986) The electron microscopical and cytochemical study on permeability of capillary in synovial membrane of rat temporomandibular joint (in Japanese). *J Jpn Oral Stomatol* **35**, 20–38.

Jain RK (2001) Normalizing tumor vasculature with anti-angiogenic therapy: a new paradigm for combination therapy. *Nat Med* **7**, 987–989.

Koch AE (2000) The role of angiogenesis in rheumatoid arthritis: recent developments. *Ann Rheum Dis* **59**(Suppl 1), i65–i71.

Li Y, Cai H, Fang W, et al. (2014) Fibroblast growth factor 2 involved in the pathogenesis of synovial chondromatosis of temporomandibular joint. *J Oral Pathol Med* **43**, 388–394.

Matsumoto T, Schiller P, Dieterich LC, et al. (2008) Ninein is expressed in the cytoplasm of angiogenic tip-cells and regulates tubular morphogenesis of endothelial cells. *Arterioscler Thromb Vasc Biol* **28**, 2123–2130.

Morikawa S, Baluk P, Kaidoh T, et al. (2002) Abnormalities in pericytes on blood vessels and endothelial sprouts in tumors. *Am J Pathol* **160**, 985–1000.

Nagashima M, Yoshino S, Ishiwata T, et al. (1995) Role of vascular endothelial growth factor in angiogenesis of rheumatoid arthritis. *J Rheumatol* **22**, 1624–1630.

Nehls V, Denzer K, Drenckhahn D (1992) Pericyte involvement in capillary sprouting during angiogenesis in situ. *Cell Tissue Res* **270**, 469–474.

Nishijima T (1981) The fine structure of the synovial membrane of the knee joint in rats with special reference to regional differences. *J Jpn Orthop Assoc* **55**, 601–613.

Nozawa-Inoue K, Takagi R, Kobayashi T, et al. (1998) Immunocytochemical demonstration of the synovial membrane in experimentally induced arthritis of the rat temporomandibular joint. *Arch Histol Cytol* **61**, 451–466.

Nozawa-Inoue K, Ohshima H, Kawano Y, et al. (1999) Immunocytochemical demonstration of heat shock protein 25 in the rat temporomandibular joint. *Arch Histol Cytol* **62**, 483–491.

Nozawa-Inoue K, Amizuka N, Ikeda N, et al. (2003) Synovial membrane in the temporomandibular joint – its morphology, function and development. *Arch Histol Cytol* **66**, 289–306.

Nozawa-Inoue K, Suzuki A, Amizuka N, et al. (2006) Expression of caveolin-1 in the rat temporomandibular joint. *Anat Rec A Discov Mol Cell Evol Biol* **288**, 8–12.

Nozawa-Inoue K, Suzuki A, Niwano M, et al. (2007) Expression of caveolin-3 in the fibroblast-like type B synoviocytes in the rat temporomandibular joint. *Anat Rec (Hoboken)* **290**, 238–242.

Ozerdem U, Stallcup WB (2003) Early contribution of pericytes to angiogenic sprouting and tube formation. *Angiogenesis* **6**, 241–249.

Paulin D, Li Z (2004) Desmin: a major intermediate filament protein essential for the structural integrity and function of muscle. *Exp Cell Res* **301**, 1–7.

Robertson RT, Levine ST, Haynes SM, et al. (2015) Use of labeled tomato lectin for imaging vasculature structures. *Histochem Cell Biol* **143**, 225–234.

Rymer C, Paredes J, Halt K, et al. (2014) Renal blood flow and oxygenation drive nephron progenitor differentiation. *Am J Physiol Renal Physiol* **307**, F337–F345.

Schwab W, Galbiati F, Volonte D, et al. (1999) Characterization of caveolins from cartilage: expression of caveolin-1, -2 and -3 in chondrocytes and in alginate cell culture of the rat tibia. *Histochem Cell Biol* **112**, 41–49.

Schwab W, Kasper M, Gavlik JM, et al. (2000) Characterization of caveolins from human knee joint cartilage: expression of caveolin-1, -2, and -3 in chondrocytes and association with integrin beta1. *Histochem Cell Biol* **113**, 221–225.

Semerano L, Clavel G, Assier I, et al. (2011) Blood vessels, a potential therapeutic target in rheumatoid arthritis? *Joint Bone Spine* **78**, 118–123.

Tsuzuki H, Sasa S (1994) Ultrastructural observation of capillary sprouts in the dental organs of rat molars. *Kaibogaku Zasshi* **69**, 684–696.

Uehara K, Miyoshi M (2002) Localization of caveolin-3 in the sinus endothelial cells of the rat spleen. *Cell Tissue Res* **307**, 329–336.

Xu B, Wu YQ, Huey M, et al. (2004) Vascular endothelial growth factor induces abnormal microvasculature in the endoglin heterozygous mouse brain. *J Cereb Blood Flow Metab* **24**, 237–244.

Supporting Information

Additional Supporting Information may be found in the online version of this article:

Fig. S1. An enlarged photo of the condyle in Fig. 1A. There is an unmineralized cartilage matrix under the hypertrophic cell layer in the chondyle.

Fig. S2. Double labeling for desmin (green) and RECA-1 (red) in the developing synovial membrane.